# MECHANICAL PROPERTIES OF MAHA SARAKHAM SALT UNDER CYCLIC LOADS

D. Phueakphum & K. Fuenkajorn

Geomechanics Research Unit, Institute of Engineering,
Suranaree University of Technology, Muang District,
Nakhon Ratchasima, Thailand 30000.
Phone (66-44) 224-758, Fax (66-44) 224-448
E-Mail: d4740056@g.sut.ac.th

**Keywords:** fatigue, creep, elasticity, strength, viscosity, salt

**ABSTRACT:** Series of laboratory testing have been performed to assess the effects of cyclic loading on compressive strength, elasticity and time-dependency of the Maha Sarakham rock salt. Results from the cyclic loading tests indicate that the salt compressive strength decreases with increasing number of loading cycles, which can be best represented by a power equation. The salt elastic modulus decreases slightly during the first few cycles, and tends to remain constant until failure. It seems to be independent of the maximum loads within the range used here. Axial strain-time curves compiled from loci of the maximum load of each cycle apparently show a time-dependent behavior similar to that of creep tests under static loading. In the steady-state creep phase, the visco-plastic coefficients calculated from the cyclic loading test are about an order of magnitude lower than those under static loading. The salt visco-plasticity also decreases with increasing loading frequency. Surface subsidence and cavern closure simulated using parameters calibrated from cyclic loading test results are about 40% greater than those from the static loading results. This suggests that application of the property parameters obtained from the conventional static loading creep test to assess the long-term stability of storage caverns in salt with internal pressure fluctuation may not be conservative.

## 1 INTRODUCTION

Rock salt around storage caverns will be subject to cycles of loading due to the fluctuation of cavern pressures during product injection and retrieval periods. Depending on the types of stored products (e.g. petroleum, liquefied gas or compressed-air) and on the designed operating schemes, the injection-withdrawal durations can range from daily to annual, and the minimum and maximum cavern pressures can be as low as 20% and as high as 90% of the in-situ stresses at the casing shoe (cavern top). Due to the complexity of cavern ground geometry and the need to predict the future stability conditions (normally up to a few decades), the stability and operating pressures of the salt caverns have commonly been analyzed and designed via numerical modeling capable of handling time-dependent constitutive equations. A difficulty may arise in determining the representative properties of the salt under such cyclic loading states. Since the salt properties are loading path dependent (non-linear), the laboratory determined properties under static loads (as commonly practiced) may not truly represent the actual in-situ salt behavior under cyclic loading.

The effect of cyclic loading on the elasticity and strengths of geologic materials has long been recognized (Haimson, 1974; Allemandou & Dusseault, 1996; Bagde & Petros, 2005). A

common goal of their studies is to determine the fatigue strength of the materials. It has been found that loading cycles can reduce the material strength and elasticity, depending on the loading amplitude and the maximum applied load in each cycle (Zhenyu & Haihong, 1990; Singh et al. 1994; Ray et al. 1999; Kodama et al., 2000). Rare investigation has however been made to identify the cyclic loading effect on the time-dependent properties and behavior of soft and creeping materials such as salt.

The objective of this research is to determine experimentally the effects of cyclic loading on compressive strength, elasticity, visco-elasticity and visco-plasticity of rock salt from the Maha Sarakham formation. The efforts primarily involve mechanical characterization testing, creep testing and compression testing under static and cyclic loads. Finite element analyses are performed to demonstrate the impact of cyclic loading on the deformation of salt around a compressed-air storage cavern.

## 2 ROCK SALT SPECIMENS

The specimens tested here have been obtained from the Lower Salt members of the Maha Sarakham formation in the Sakhon Nakhon basin, northeastern Thailand. This salt unit is being considered as a host rock for compressed-air energy storage by the Thai Department of Energy. The rock salt is relatively pure halite with slight amount (less than 1-2%) of anhydrite, clay minerals and ferrous oxide. The average crystal (grain) size is about 5×5×10 mm. Warren (1999) gives detailed descriptions of the salt and geology of the basin. The core specimens with a nominal diameter of 60 mm tested here were drilled from depths ranging between 250 and 400 meters.

Sample preparation followed the ASTM (D4543) standard practice, as much as practical. Twenty-four specimens (L/D = 2.5) were prepared for uniaxial compression tests, 76 specimens (L/D of 0.5) for Brazilian tension tests, 14 specimens (L/D = 2.5) for cyclic loading tests, and 10 specimens (L/D = 2.5) for uniaxial creep tests. The samples were cut and ground using saturated brine as lubricant. After preparation, the specimens were labeled and wrapped with plastic film. The specimen designation was identified. Prior to mechanical testing, visual examination was made to determine the type and amount of inclusions.

## 3 CHARACTERIZATION TESTING

Uniaxial and triaxial compression and Brazilian tension tests have been conducted to obtain data for the Maha Sarakham salt, and to determine the test parameters for the subsequent creep and cyclic loading tests. The test procedure follows relevant ASTM standard practices (ASTM D3967 and D7012). The elastic modulus (measured from unloading curves) of the salt is 25.2±1.9 GPa and the Poisson's ratio is 0.37±0.11. The uniaxial compressive and Brazilian tensile strengths are 34.7±2.2 MPa and 1.5±0.4 MPa. Figure 1 shows the stress-strain curves monitored during the tests. The triaxial compressive strength tests use confining pressures between 5.5 and 19.3 MPa. Based on the Coulomb criterion the internal friction angle is calculated as 52 degrees and the cohesion as 6 MPa (Figure 2). The Maha Sarakham salt strengths and elasticity obtained here agree reasonably well with those obtained elsewhere (e.g., Hansen et al., 1984).

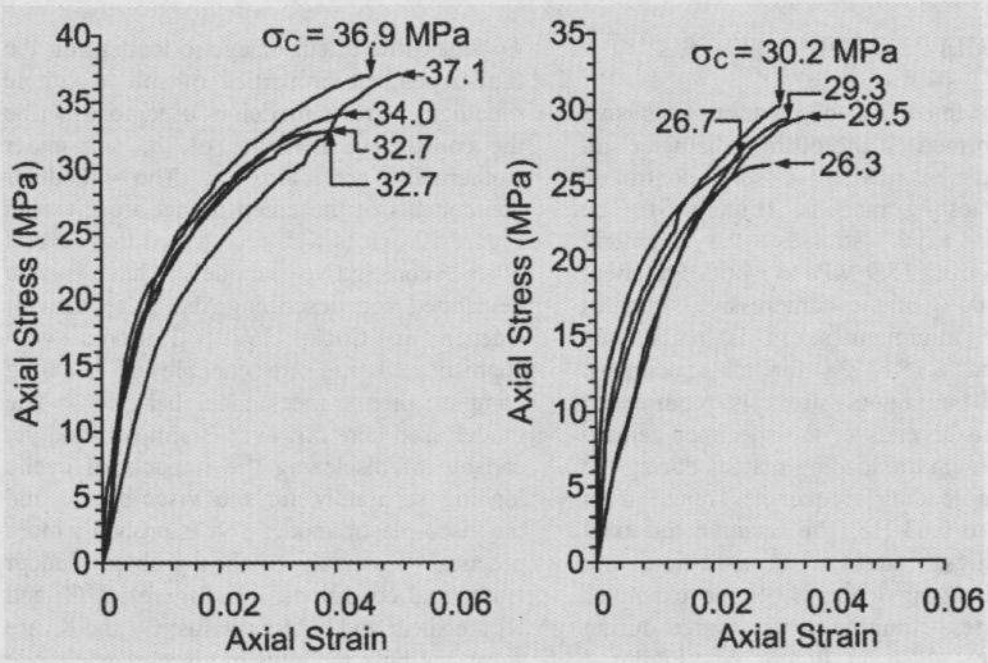


**Figure 1.** Results of uniaxial compressive strength testing. Numbers indicate stress at failure.

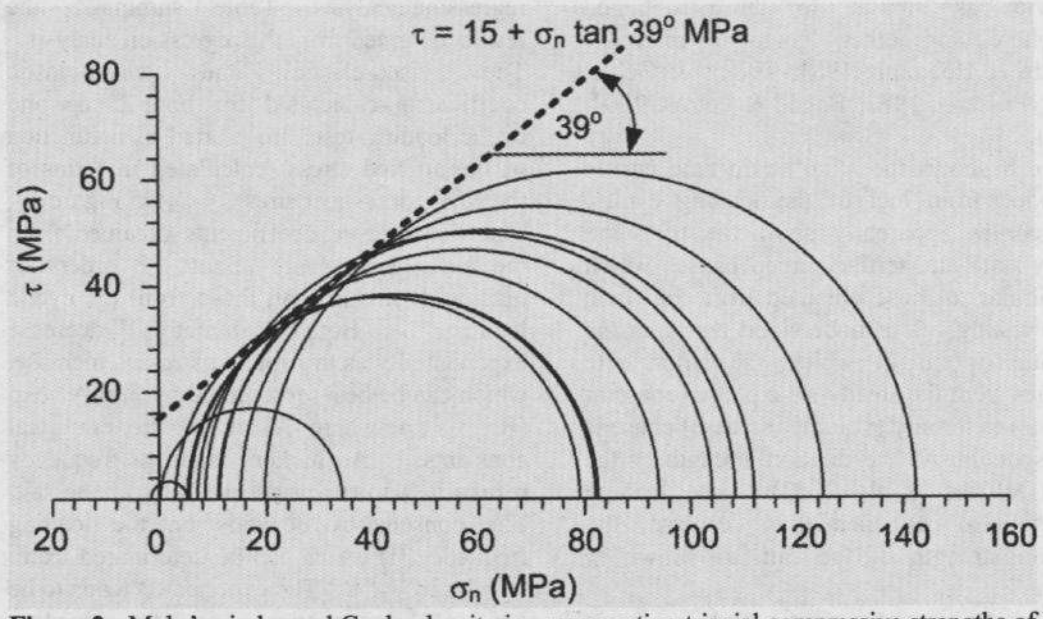


**Figure 2.** Mohr's circles and Coulomb criterion representing triaxial compressive strengths of Maha Sarakham Salt.

## 4 CREEP TESTING

Short- and long-term uniaxial creep tests have been performed to determine the time-dependent properties of the salt under isothermal condition. The test procedure follows the ASTM D7070-08 standard practice. The short-term test results are used to calibrate the visco-elastic parameters, and the long-term results calibrate the visco-plastic coefficient of the salt. For the uniaxial testing, the applied constant axial stresses vary from 10 to 30 MPa for the short-term testing, and from 7.8 to 12.6 MPa for the long-term testing. Figures 3 and 4 plot the axial strain as a function of time for the short- and long-term testing.

## 5 CYCLIC LOADING TESTS

A series of uniaxial cyclic loading tests have been performed on the 60 mm diameter salt core specimens using a servo-controlled universal testing machine (Figure 5). The maximum axial stresses vary among specimens from 15.9 MPa to 34.6 MPa (about 40% to 100% of the compressive strength) while the minimum stress is maintained constant at 0.15 MPa for all specimens. This small minimum stress is required to ensure that the ends of the specimen remain in contact with the loading platens during the test. The loading frequencies range from 0.001 Hz to 0.03 Hz. The accumulated axial strain, fatigue stress (S) and time are monitored during loading. Some examples of axial stress-strain curves measured during loading are given in Figure 6. Figure 7 shows the decrease of the failure (fatigue) stress as the number of loading cycle (N) increases, which can be represented by a power equation: $S = 32.33\ N^{(-0.07)}$. The behavior is similar to those obtained elsewhere for other geologic materials (Costin & Holcomb, 1981; Thoms & Gehle, 1982; Passaris, 1982; Bagde & Petros, 2004, 2005).

Figure 8 shows the axial strain-time curves compiled from loci of the loading cycles. The curves apparently show the transient, steady-state and tertiary creep phases which are similar to those obtained from the static creep testing. It is understood here that the transition point at which the strain rate changes from the steady-state phase (constant volume) to tertiary (volume increase) phase is corresponding to the dilation strength of the salt (DeVries et al., 2003). The loading cycles also exponentially decrease the dilation strength of the salt, as shown in Figure 7.

For each specimen the elastic modulus values calculated from the series of unloading curves are plotted as a function of loading cycles in Figure 9. For all stress levels, the salt elasticity exponentially decreases as the number of loading cycles increases, and remains constant after about 50 to 100 cycles. The calculated elastic modulus values range from 20 GPa to 35 GPa. They however tend to be independent of the applied maximum loads used here.

## 6 SALT PROPERTY CALIBRATION

To assess the effect of cyclic loading on the time-dependent properties of salt, a simple rheological creep model is used to describe the constitutive behavior of the salt under isothermal condition. The modular components of the creep model are given in Figure 10. It is well recognized that several other constitutive models have been developed for describing the salt behavior (Jaeger & Cook, 1979). Some very sophisticated and are capable of handling complex thermo-mechanical behavior. The model used here however is simpler, and yet capable of disclosing the impacts of cyclic loading separately for the visco-elastic and the visco-plastic modes. It is probably more practical to analyze the problem under isothermal conditions. In Figure 10, $G_1$ and $K_1$ are shear and bulk modulus; $G_2$ and $K_2$ are shear and bulk modulus in visco-elastic mode; and $\eta_2$ and $\eta_4$ are visco-elastic and visco-plastic coefficients. These elastic and time-dependent parameters can be calibrated from the laboratory test results using a regression analysis. Table 1 summarizes the results obtained from the regression analysis.

The visco-elastic and visco-plastic coefficients calculated for both creep and cyclic loading tests are plotted as a function of the applied stress (calculated in terms of the octahedral shear stress, $_{oct}$) in Figure 11. The visco-plastic coefficients obtained from the creep testing are about 1-2 orders of magnitude higher than those from the cyclic loading. Both parameters decrease exponentially as the applied stresses increase, which can be best represented by: $\eta = A \cdot \exp(B \cdot {}_{oct})$, where A and B are empirical constants. A higher loading frequency results in a lower visco-plasticity of the salt. The constant A depends on the loading frequency (f) which can be determined from: $A = 25.2 \cdot f^{(-0.18)}$. The exponent B tends to be constant, independent of the loading frequency range used here (Table 2).

The axial strain-time curves obtained from the cyclic loading (as shown in Figure 8) also yield the critical octahedral shear strain ( $_c$) for the salt. These strains correspond to the transition point from plastic creep (no volume change) in steady-state phase to dilation (volume increase) in the tertiary phase. The critical shear strain decreases exponentially with increasing octahedral shear stress. Figure 12 plots the measured $_c$ as a function of $_{oct}$, and shows their empirical relation.

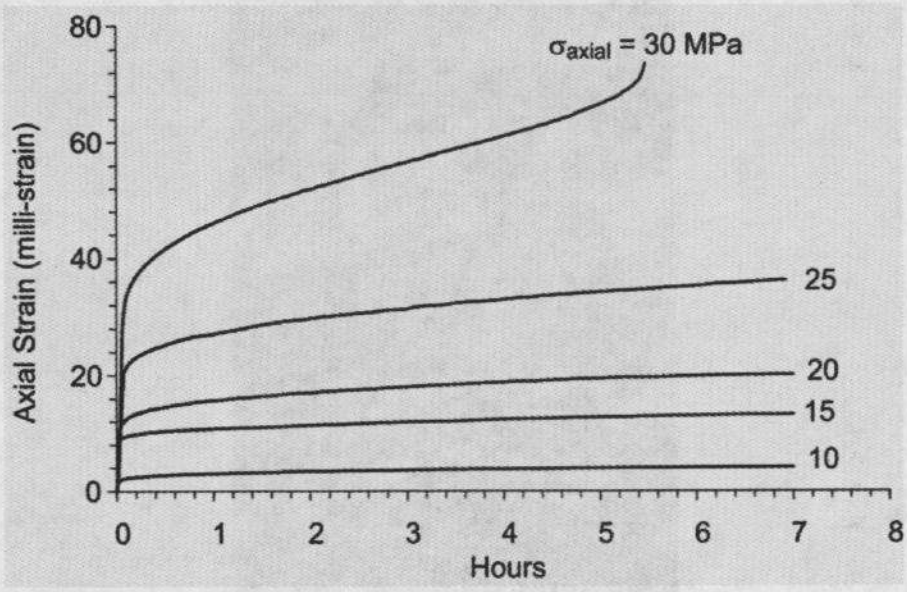


**Figure 3.** Results of the short-term uniaxial creep tests.

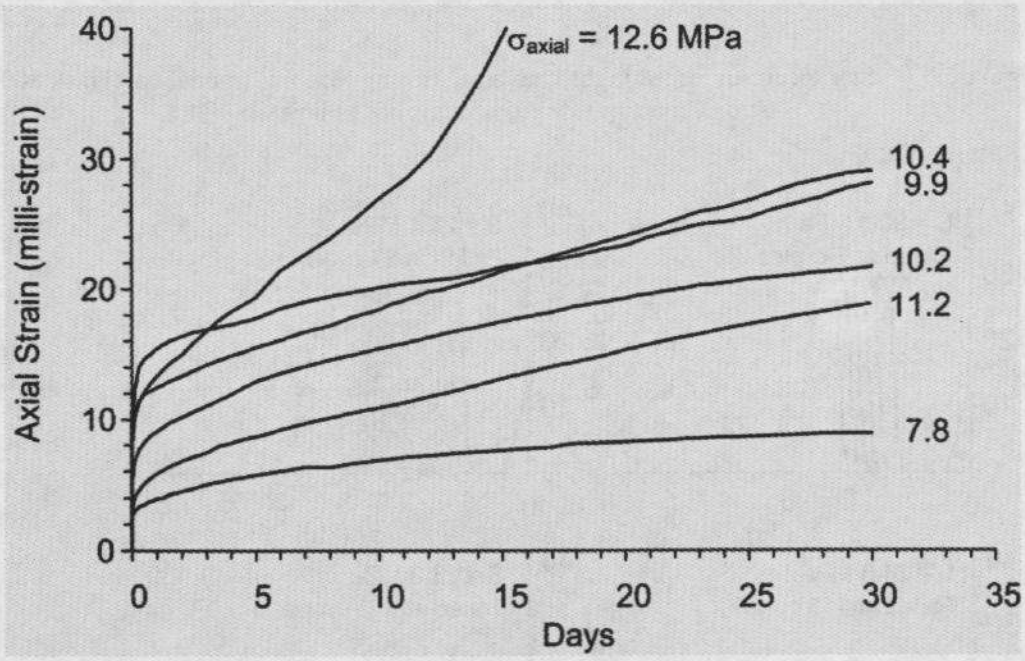


**Figure 4.** Results of the long-term uniaxial creep tests.

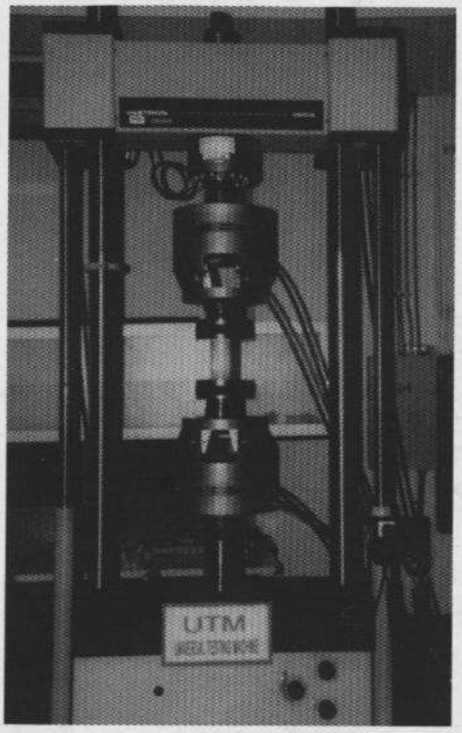


**Figure 5.** Salt specimen placed in the Universal Testing Machine (model FastTrack 8800, Instron Company) for uniaxial cyclic loading test.

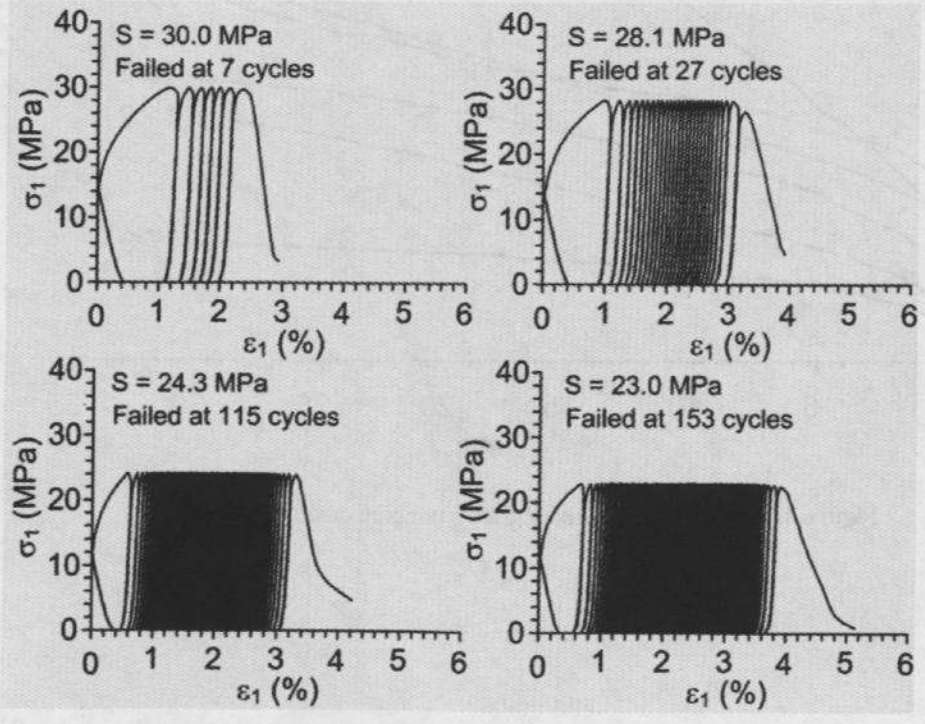


**Figure 6.** Examples of cyclic loading test results. Axial stress ( $_1$) plotted as a function of axial strain ( $_1$). We can not explain why the machine records the decrease of axial strain in the first cycle.

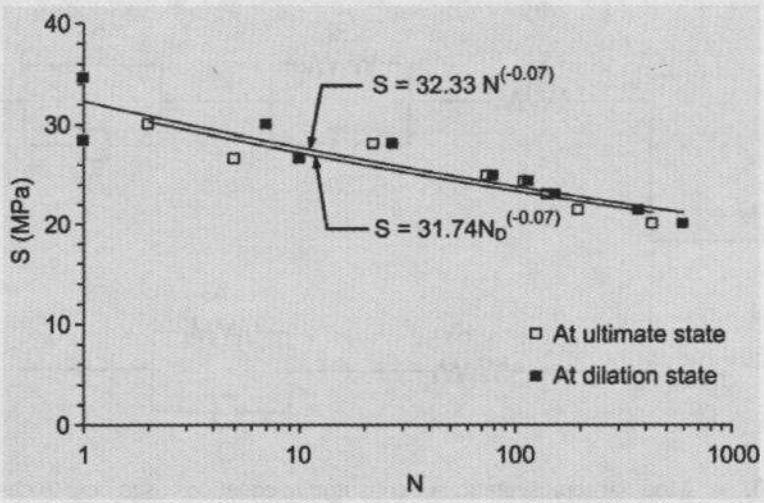


**Figure 7.** Fatigue strength (S) plotted as a function of numbers of loading cycles at failure (N) and at dilation ($N_D$).

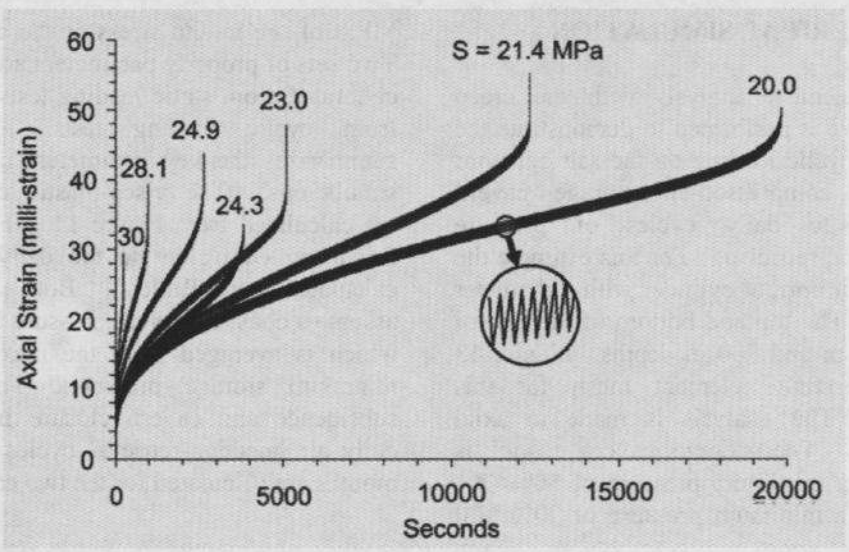


**Figure 8.** Axial strain-time curves from uniaxial cyclic loading tests.

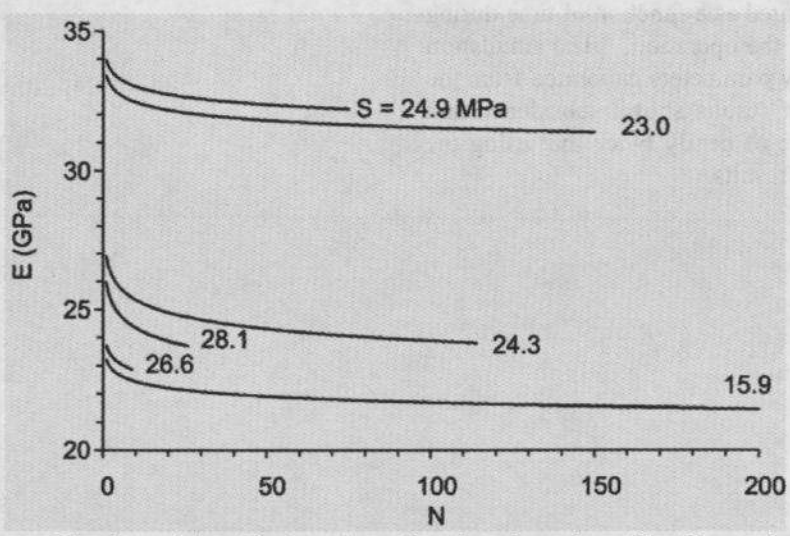


**Figure 9.** Elastic modulus (E) plotted as a function of number of loading cycles (N) up to failure.

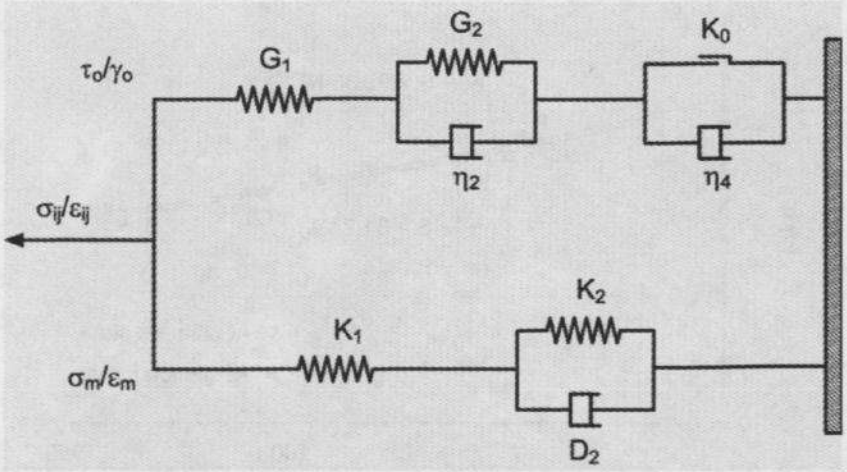


**Figure 10.** Modular representation of constitutive equations used here to describe the time-dependent behavior of salt (modified from Fuenkajorn & Serata, 1994).

## 7 NUMERICAL SIMULATION

A finite element analysis with the creep model above is performed to demonstrate the impact of cyclic loading on the salt behavior around a compressed-air storage cavern subjecting to daily cycles of pressure injection and retrieval. For this example the cavern is an upright cylinder with a diameter of 50 m. The top and bottom of the cavern are at 500 m and 700 m depths. Figure 13 shows the finite element mesh for this example. The analysis is made in axial symmetry. The storage cavern model is subject to a maximum pressure of 80% (8.1 MPa) and a minimum pressure of 20% (2.0 MPa) of the in-situ stress at the cavern top. Two sets of property parameters are used, one calibrated from static loading tests, the other from cyclic loading tests. Table 3 summarizes the key parameters used in the simulations. The visco-plastic coefficients are calculated from Figure 11. The loading frequency equivalent to the daily cycles is calculated from Table 2. Both simulations assume a constant cavern pressure of 5.1 MPa which is averaged from the maximum and minimum storage pressures. The surface subsidence and cavern closure induced by daily air injection-retrieval cycles during 12 months are calculated for the two cases.

Figure 14 shows the surface subsidence (above the center of the cavern) and cavern closure computed as a function of time during 12 months of the operation. The simulation using property parameters calibrated from the cyclic loading results shows subsidence and cavern closure of nearly twice that using the static loading results.

**Table 1.** Visco-elastic and visco-plastic coefficients obtained from creep and cyclic loading tests

| Test Methods | $\eta_1$ (MPa) | $\tau_{oct}$ (MPa) | $\sigma_{mean}$ (MPa) | $\eta_2$ (GPa.day) | $\eta_4$ (GPa.day) |
|---|---|---|---|---|---|
| Uniaxial creep test | 7.8 | 3.7 | 2.6 | 1.2 | 29.1 |
| | 9.9 | 4.7 | 3.3 | 0.3 | 8.8 |
| | 10.2 | 4.8 | 3.4 | 1.0 | 8.7 |
| | 11.2 | 5.3 | 3.7 | 1.0 | 8.9 |
| | 11.4 | 5.4 | 3.8 | 0.7 | 7.4 |
| | 4.1 | 1.9 | 1.4 | - | 83.3 |
| | 7.1 | 3.3 | 2.4 | - | 53.4 |
| | 9.1 | 4.3 | 3.0 | - | 16.6 |
| | 11.1 | 5.2 | 3.7 | - | 12.1 |
| | 14.1 | 6.6 | 4.7 | - | 3.5 |
| Cyclic loading test (f = 0.03 Hz) | 20.0 | 9.4 | 6.7 | 0.011 | 0.064 |
| | 21.4 | 10.1 | 7.1 | 0.010 | 0.041 |
| | 23.0 | 10.8 | 7.7 | 0.006 | 0.022 |
| | 24.3 | 11.5 | 8.1 | 0.003 | 0.015 |
| | 24.9 | 11.7 | 8.3 | 0.003 | 0.012 |
| | 28.1 | 13.2 | 9.4 | 0.001 | 0.005 |
| | 30.0 | 14.1 | 10.0 | - | 0.002 |
| Cyclic loading test (f = 0.001 Hz) | 16.0 | 7.5 | 5.3 | - | 0.355 |
| | 21.6 | 10.2 | 7.2 | - | 0.075 |
| | 23.0 | 10.8 | 7.7 | - | 0.053 |
| | 27.0 | 12.7 | 9.0 | - | 0.010 |
| | 29.0 | 13.7 | 9.7 | - | 0.005 |

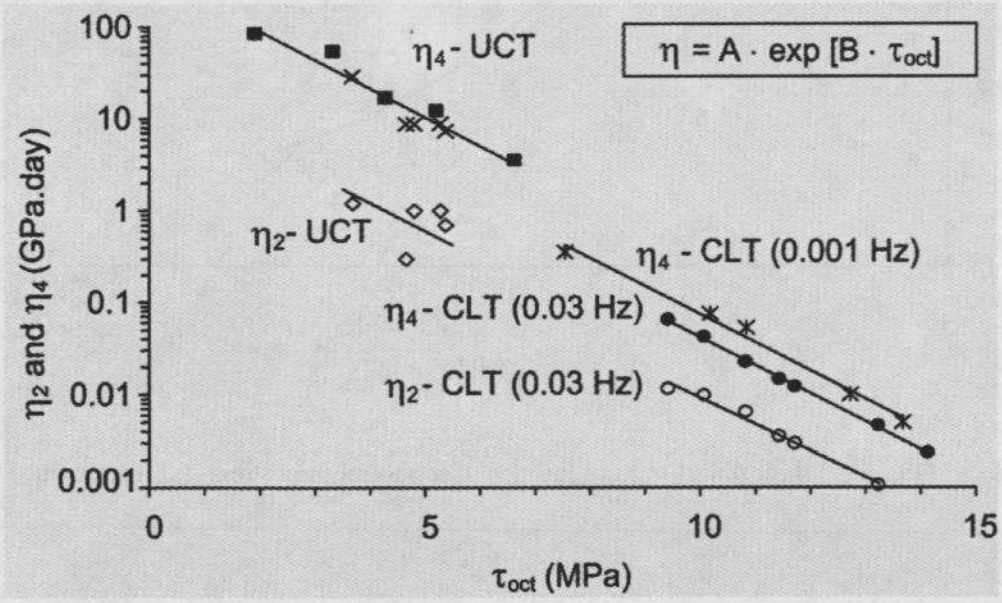


**Figure 11.** Visco-elasticity ( $\eta_2$) and visco-plasticity ( $\eta_4$) as a function of octahedral shear stress ( $\tau_{oct}$) obtained from creep tests (UCT) and cyclic loading tests (CLT).

**Table 2.** Constants A and B for empirical equation: $\eta = A \exp [B. \tau_{oct}]$.

| Viscosity Coefficients | Frequency f (Hz) | A | B |
|---|---|---|---|
| Uniaxial Creep Test (UCT): | | | |
| - Visco-plasticity ( $_4$) | $0.19\times10^{-6}$ | 382 | -0.72 |
| - Visco-elasticity $_2$) | $0.19\times10^{-6}$ | 21 | -0.72 |
| Uniaxial Cyclic Loading Test (CLT): | | | |
| - Visco-plasticity ( $_4$): | 0.001 | 87 | -0.71 |
| - Visco-plasticity ( $_4$): | 0.03 | 46 | -0.70 |
| - Visco-elasticity ( $_2$): | 0.03 | 7 | -0.66 |
| Predicted $_4$: | | | |
| - Daily cycle | $11.6\times10^{-6}$ | 190* | -0.70 |
| - Monthly cycle | $0.39\times10^{-6}$ | 356* | -0.70 |

* Predicted by using the following equation: $A = 25.2\ f^{(-0.18)}$

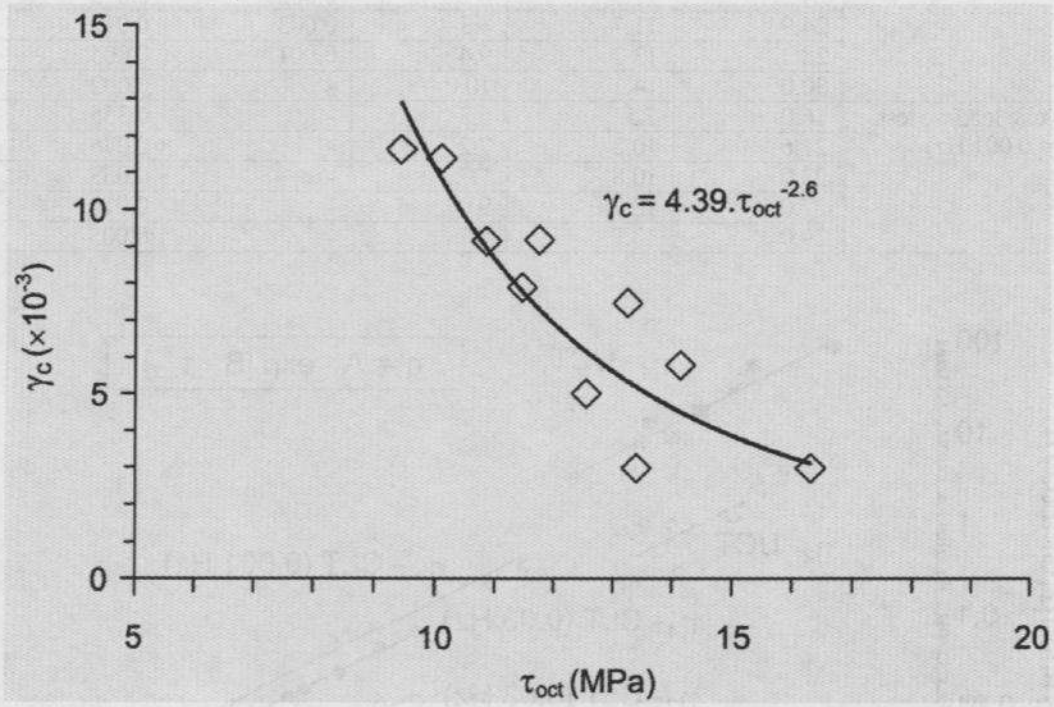


**Figure 12.** Octahedral shear strain ( $_c$) as a function of octahedral shear stress ( $_{oct}$) determined from cyclic loading tests.

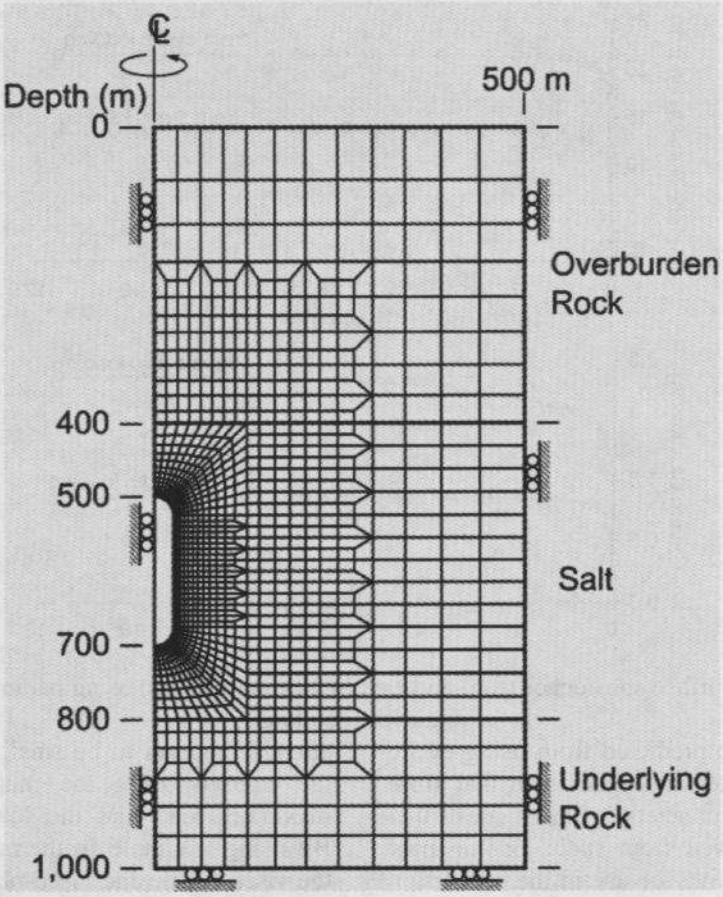


**Figure 13.** Finite element mesh constructed to simulate an example of storage cavern in salt.

**Table 3.** Summary of property parameters used in numerical simulation

| Key Properties | Static Loading | Cyclic Loading |
|---|---|---|
| Elastic Parameters | | |
| Elastic Modulus, E (MPa) | 25.2 | 25.2 |
| Poisson's Ratio, $\nu$ | 0.37 | 0.37 |
| Shear Modulus, $G_1$ (GPa) | 10.2 | 10.2 |
| Bulk Modulus, $K_1$ (GPa) | 39.2 | 39.2 |
| Visco-elastic and Visco-plastic Parameters | | |
| Visco-elastic Shear Modulus, $G_2$ (GPa) | 1.0 | 0.8 |
| Visco-elastic Bulk Modulus, $K_2$ (GPa) | 3.8 | 2.9 |
| Visco-elastic Coefficient, $_2$ (GPa.day) | 0.5 | 0.3 |
| Visco-elastic Plastic Coefficient, $_4$ (GPa.day) | 3.4 | 1.8 |
| Critical Octahedral Shear Strain, $\gamma_c$ ($\times 10^{-3}$) | 5 | 2 |

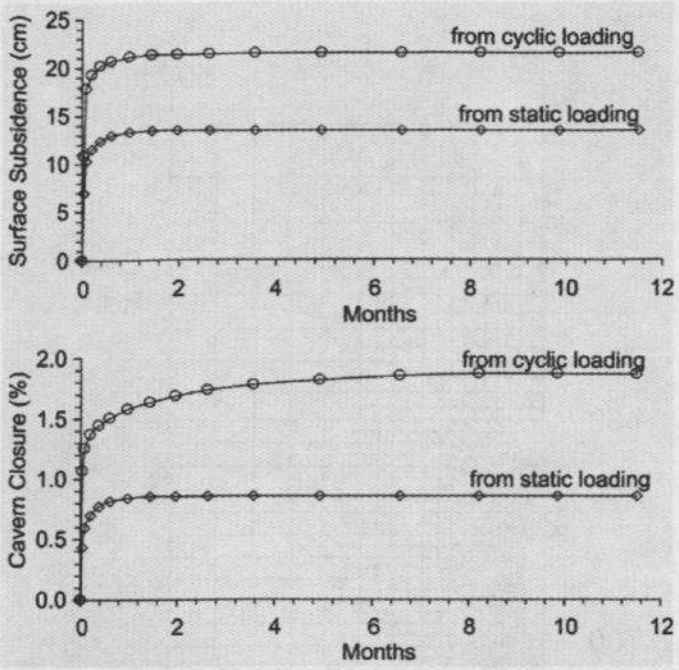


**Figure 14.** Surface subsidence (top) and cavern closure (bottom) using parameters from static and cyclic loading.

The closure rate predicted from using cyclic loading parameters is higher than that from static loading parameters. This suggests that parameters derived from static loading may not be conservative for use in the simulation of salt storage caverns that are subject to repeated change of the internal pressure.

## 8 DISSCUSSIONS AND CONCLUSIONS

The uniaxial cyclic loading tests as conducted here not only provide the fatigue stress and complete strain-time curves of the salt, but also reveal the dilation strength and critical shear strain of the rock. These parameters can not be easily obtained from the conventional test methods (i.e., the compressive strength test and creep test). The fatigue stress can help defining the operational life of storage caverns in salt, which depends also on the loading cycles and the loading amplitudes (difference between the maximum and minimum storage pressures). The creep (viscosity) parameters are necessary to determine the time-dependent deformation of the surrounding salt. The critical strain and dilation strength define the maximum deformation before dilation strain or accelerated creep rate occur under a given shear stress. This is useful for the design of the safe minimum internal pressure for a gas or compressed-air storage cavern in salt.

Under the test parameters used here the cyclic loading can decrease the salt strength by up to 30%, depending on the maximum applied load and the number of loading cycles. The effect of loading frequency on the salt strength appears to be small as compared to the impacts from the magnitudes of the maximum load and the loading amplitude. By using a simple isothermal creep model, the visco-elastic and visco-plastic coefficients of the salt can be determined from the static and the cyclic loading test results. Both parameters decrease exponentially with increasing applied octahedral shear stress. They also decrease with increasing loading frequency. The results from storage cavern simulations suggest that the property parameters obtained from the static (creep) tests can under-estimate the cavern deformation and surface subsidence as compared to those from the cyclic loading tests. This could lead to a non-conservative cavern design and stability analysis. The effect of loading frequency on the elastic modulus of the salt can not be detected here. This is probably because of the narrow range of the tested frequencies or the intrinsic variability among the salt specimens, or both.

## AKNOWLEDGEMENT

This research is funded by Suranaree University of Technology. Permission to publish this paper is gratefully acknowledged.

## REFERENCES

Allemandou, X. & Dusseault, M.B., 1996. Procedures for cyclic creep testing of salt rock, results and discussions. In Ghoreychi, M., Berest, P., Hardy, H.R. & Langer, M. (eds.), Proceeding of the

Third Conference on the Mechanical Behavior of Salt, 14-16 September 1993. Clausthal-Zellerfeld: Trans Tech Publications, pp. 207-218.

ASTM D3967-86. Standard test method for splitting tensile strength of intact rock core specimens. Annual Book of ASTM Standards, Vol. 04.08. Philadelphia, PA: ASTM.

ASTM D4543-08. Standard practice for preparing rock core specimens and determining dimensional and shape tolerances. Annual Book of ASTM Standards, Vol. 04.08. West Conshohocken, PA: ASTM.

ASTM D7012-07. Compressive strength and elastic moduli of intact rock core specimens under varying states of stress and temperatures. Annual Book of ASTM Standards, Vol. 04.08. West Conshohocken, PA: ASTM.

ASTM D7070-08. Creep of rock core under constant stress and temperature. Annual Book of ASTM Standards, Vol. 04.08. West Conshohocken, PA: ASTM.

Bagde M.N. & Petros, V., 2004. Experimental investigation into fatigue behaviour of intact sandstone and conglomerate rock types in uniaxial dynamic cyclic loading. Geophysical Research Abstracts, 6: 07240.

Bagde, M.N. & Petros, V., 2005. Fatigue properties of intact sandstone samples subjected to dynamic uniaxial cyclical loading. International Journal of Rock Mechanics and Mining Sciences, 42(2): 237-250.

Costin, L.S. & Holcomb, D.J., 1981. Time-dependent failure of rock under cyclic loading. Tectonophysics, 79(3-4): 279-296.

DeVries, K.L., Mellegard, K.D. and Callahan, G.D., 2003. Laboratory testing in support of a bedded salt failure criterion. SMRI: Fall 2003 meting, 5-8 October 2003, Chester, United Kingdom, England.

Fuenkajorn, K. & Serata, S., 1994. Dilation-induced permeability increase around caverns in rock salt. In Proc. 1st North American Rock Mechanics Symposium, 1-3 June. University of Texas at Austin, A.A Balkema, Rotterdam. pp. 648-656.

Haimson, B.C., 1974. Mechanical behavior of rock under cyclic loading. In Proceedings of the 3rd Congress of the International Society for Rock Mechanics, Part A. Advances in Rock Mechanics: Report of Current Research, 1-7 September. National Academy of Sciences: Washington, D.C., pp. 373-387.

Hansen, F.D., Mellegard, K.D. & Senseny, P.E., 1984. Elasticity and strength of ten natural rock salts. In Proceeding of the 1st Conference on the Mechanical Behavior of Salt. Trans Tech Publications: Clausthal Germany, pp. 71-83.

Jaeger, J.C. and Cook, N.G.W., 1979. Fundamentals of Rock Mechanics. 3rd edition, Chapman and Hall, London.

Kodama, J., Ishizuka, Y., Abe, T., Ishijima, Y. & Goto, T., 2000. Estimate of the fatigue strength of granite subjected to long-period cyclic loading. Shigen-to-Sozai, 116: 111-118.

Passaris, E.K.S., 1982. Fatigue characteristics of rock salt with reference to underground storage caverns. In Proceeding ISRM Symposium, Rock Mechanics: Caverns and Pressure Shafts, 26-28 May. Aachen, pp. 983-989.

Ray, S.K., Sarkar, M. & Singh, T.N., 1999. Effect of cyclic loading and strain rate on the mechanical behaviour of sandstone. International Journal of Rock Mechanics and Mining Sciences, 36(4): 543-549.

Singh, T.N., Ray, S.K. & Singh, D.P., 1994. Effect of uniaxial cyclic compression on the mechanical behaviour of rocks. Indian Journal of Engineering & Materials Sciences, 1(2): 118-120.

Thoms, R.L. & Gehle, R., 1982. Experimental study of rock salt for compressed air energy storage. In ISRM Symposium, Rock Mechanics: Caverns and Pressure Shafts, 26-28 May 1982. Aachen, pp. 991-1002.

Warren, J., 1999, Evaporites: Their Evolution and Economics. Blackwell Science. Oxford.

Zhenyu, T. & Haihong, M., 1990. An experimental study and analysis of the behaviour of rock under cyclic loading. International Journal of Rock Mechanics & Mining Sciences, 27(1): 51-56.